

B₃S₂ monolayer as an anode material for Na/K-ion batteries: a first-principles study

Danhong Wang,^a Zhifang Yang,^a Wenliang Li,^{*a} Jingping Zhang^{*a}

Table of contents

Fig. S1. The phonon dispersion of B ₃ S ₂ monolayer using a (2x2x1) cell.	P1
Fig. S2. (a) Electronic band structure and (b) DOS of B ₃ S ₂ monolayer using a (2x2x1) cell.	P1
Fig. S3. Electronic band structures and DOSs of B ₃ S ₂ monolayer after the adsorption of Li, Na, and K atoms.	P2
Fig. S4. Top and side views of geometric structures for Li adsorption on the B ₃ S ₂ monolayer.	P3
Fig. S5. The lattice constant variation as the function of Na and K concentration x: (a) Na _x B ₃ S ₂ , (b) K _x B ₃ S ₂ .	P3
Fig. S6. Snapshots of (a) Na ₆ B ₃ S ₂ and (b) K ₂ B ₃ S ₂ equilibrium structures at 300 K at the end of 2 ps AIMD simulations.	P4

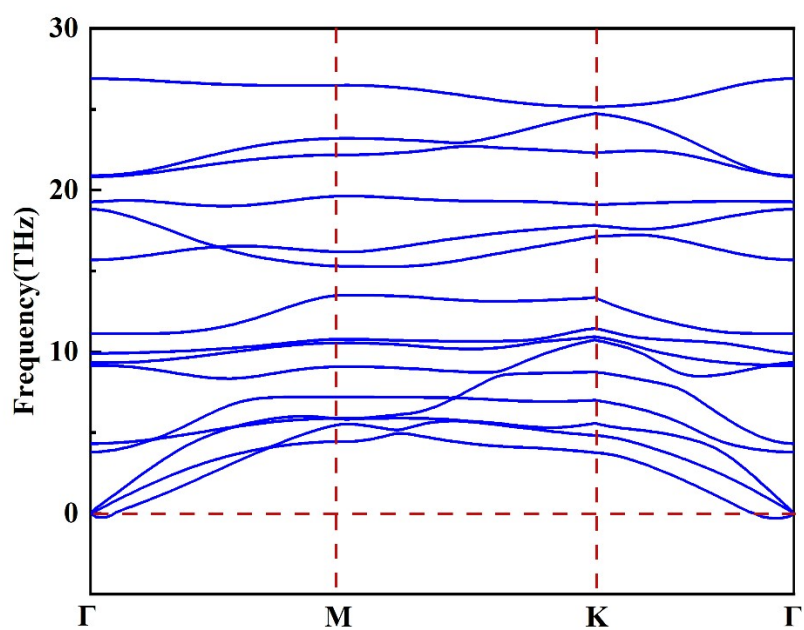


Fig. S1. The phonon dispersion of B_3S_2 monolayer using a $(2 \times 2 \times 1)$ cell.

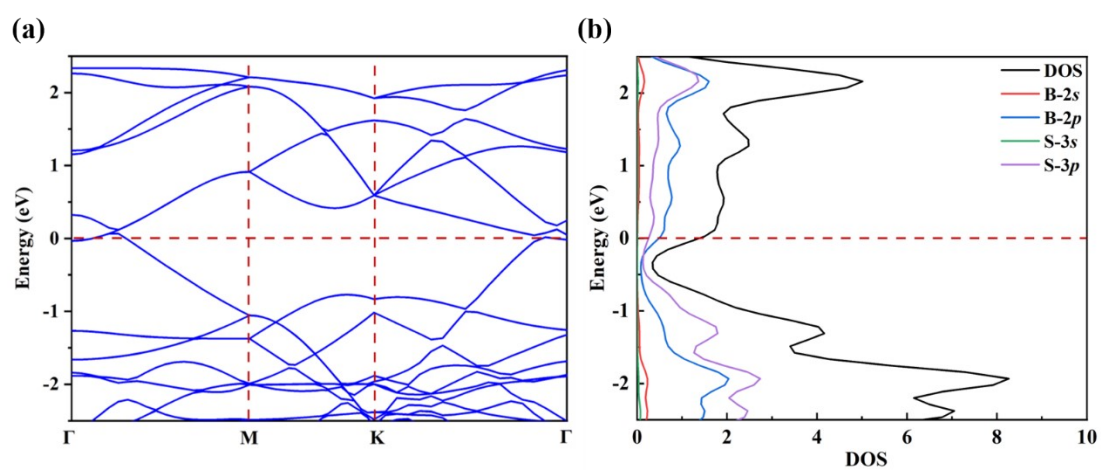


Fig. S2. (a) Electronic band structure and (b) DOS of B_3S_2 monolayer using a $(2 \times 2 \times 1)$ cell.

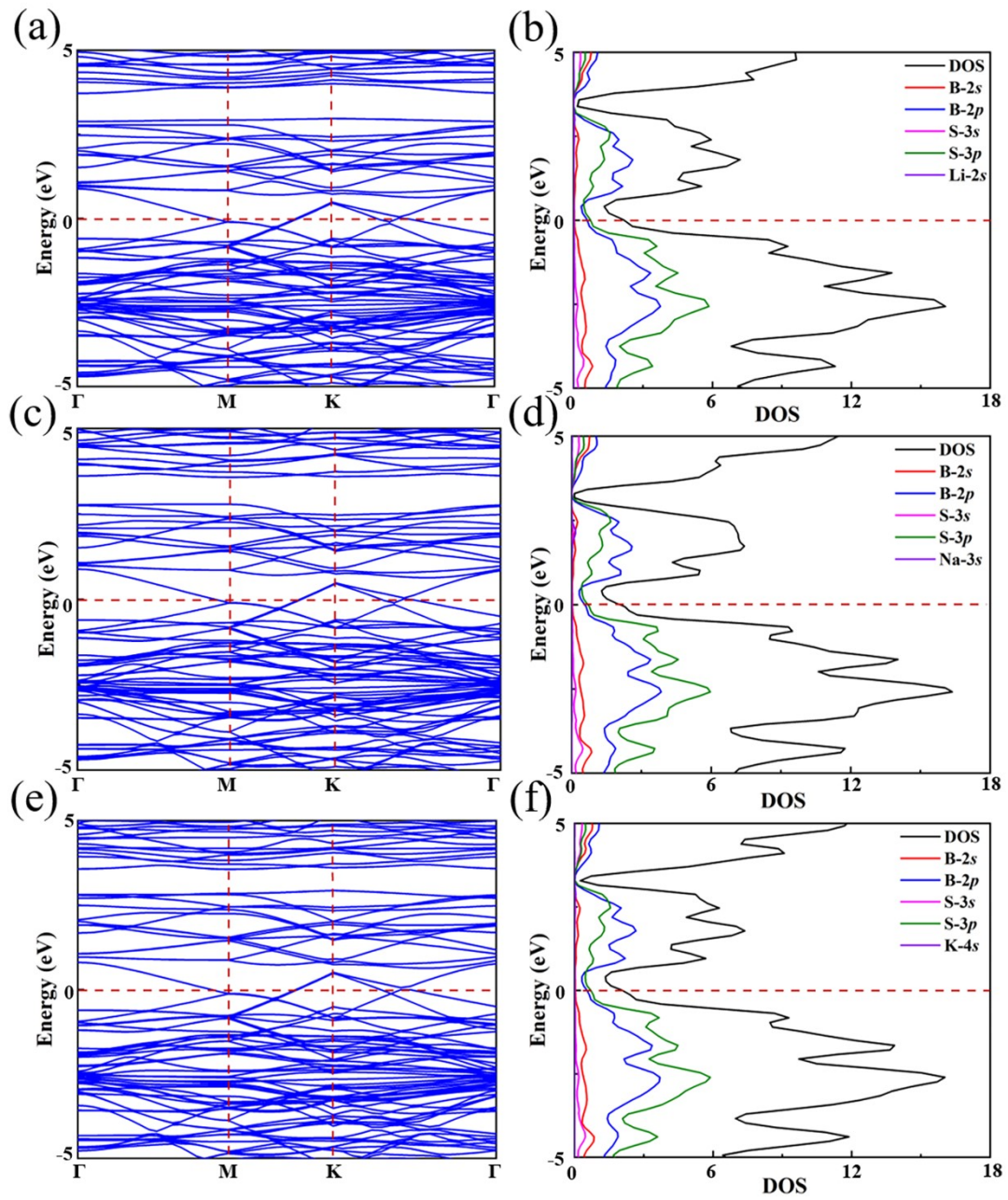


Fig. S3. Electronic band structures and DOSs of B_3S_2 monolayer after the adsorption of Li, Na, and K atoms.

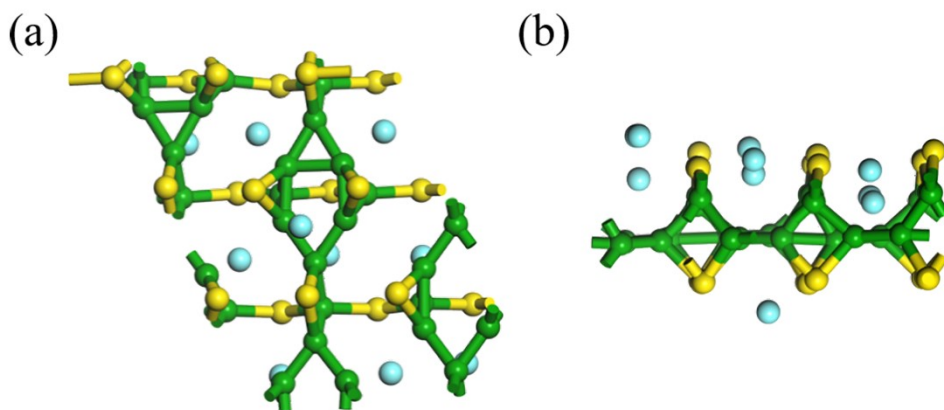


Fig. S4. Top and side views of geometric structures for Li adsorption on the B_3S_2 monolayer.

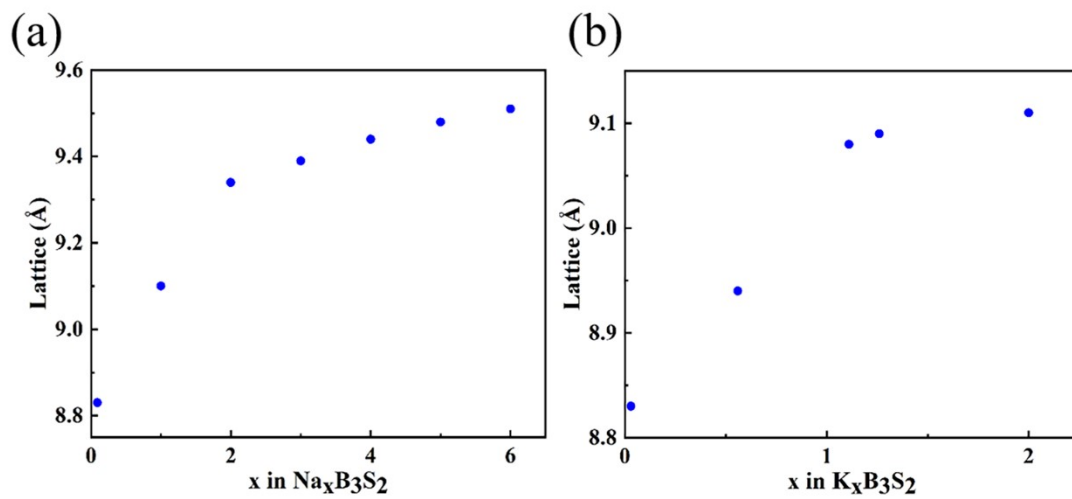


Fig. S5. The lattice constant variation as the function of Na and K concentration x : (a) $Na_xB_3S_2$, (b) $K_xB_3S_2$.

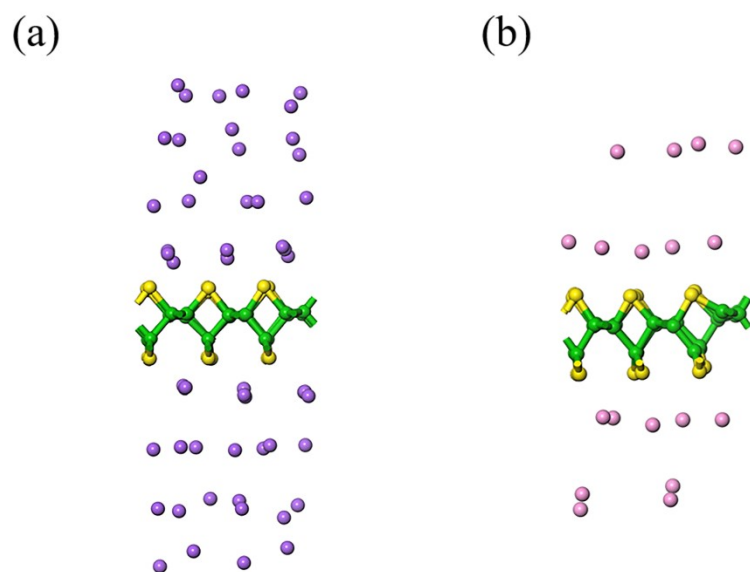


Fig. S6. Snapshots of (a) Na₆B₃S₂ and (b) K₂B₃S₂ equilibrium structures at 300 K at the end of 2 ps AIMD simulations.